ACS APPLIED MATERIALS & INTERFACES

RESEARCH ARTICLE

www.acsami.org

Effect of Catalyst Layer Density and Growth Temperature in Rapid Atomic Layer Deposition of Silica Using Tris(*tert*-pentoxy)silanol

Seok-Jun Won,[†,§] Joon Rae Kim,[†] Sungin Suh,[†] Nae-In Lee,[§] Cheol Seong Hwang,[*,†,‡] and Hyeong Joon Kim[*,†]

[†]Department of Materials Science and Engineering and [‡]WCU Hybrid Materials Program, Inter-University Semiconductor Research Center, Seoul National University, 599 Gwanak-ro, Gwanak-gu, Seoul 151-742, Republic of Korea

[§]Advanced Process Development Team, System-LSI Division, Samsung Electronics Co., Ltd., San no. 24, Nongseo-Dong, Kiheung-Gu, Yongin-City, Kyungki-Do 449-900, Republic of Korea

ABSTRACT: Rapid atomic layer deposition (RALD) of SiO_2 thin films was achieved using trimethyl-aluminum and tris(*tert*-pentoxy)silanol (TPS) as the catalyst and Si precursor, respectively. A maximum growth rate as high as ~28 nm/cycle was obtained by optimizing the catalyst layer density, whereas the previous reports showed lower values of 12 to 17 nm/cycle [Hausmann et al. *Science* **2002**, *298*, 402−406; Burton et al. *Chem. Mater.* **2008**, *20*, 7031−7043]. When the growth temperature was increased from 140 to 230 °C, the growth rate was not much reduced and the TPS pulse time showing a saturated growth rate became rather longer. Si−CH_3, Si−OH, and Si−H bonds were not detected in infrared spectra from the RALD SiO_2 film grown at 230 °C. The film quality could be enhanced substantially by applying a higher growth temperature and an in situ post plasma treatment process.

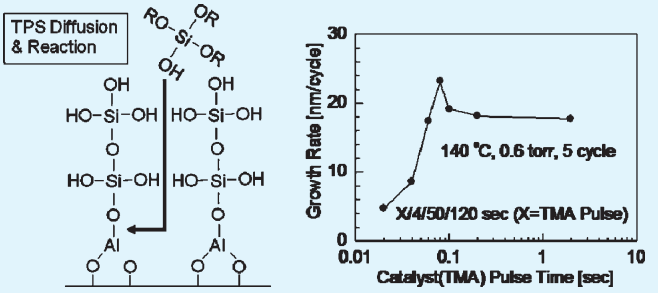

KEYWORDS: atomic layer deposition, silicon oxide, growth rate, catalyst, siloxane

INTRODUCTION

In atomic layer deposition (ALD), the film thickness can be controlled on an atomic scale by the alternating injection of a precursor and reactant gas and the self-limiting film growth behavior where the only chemically adsorbed precursors remain on the surface after the purge step.[1,2] From the mechanism, ALD has distinguishing properties of a low growth temperature, high film quality, and excellent step coverage, and has been used in many applications.[3−15] However, the process generally has very low growth thickness per cycle (usually, 0.05−0.2 nm/cycle) due to layer-by-layer growth. The typical growth rates of ALD range from 0.1 to 12 nm/min because one ALD cycle normally takes 1−30 s. In the semiconductor industry, the processing time of a wafer needs to be <5 min. Therefore, conventional ALD methods are unsuitable for depositing films of >50 nm in thickness. For this reason, many studies have been carried out to obtain higher growth rates in ALD.

Recently, a new concept ALD was introduced (called rapid ALD, RALD) for the growth of SiO_2 film with a very high growth rate of >100 times that of conventional ALD.[17] Hausmann et al. first reported the results of RALD of SiO_2 thin films. In the RALD, tris(tert-butoxy)silanol (TBS) was used as a Si precursor and a well-known Al precursor, trimethyl-aluminum (TMA), was used as a catalyst to deposit SiO_2 thin films.[16] In this process, as shown schematically in Figure 1a and b, an Al catalyst monolayer is formed by a TMA single pulse and a silicon oxide film is self-constructed by providing the Si precursor without a reactant gas. There are two important aspects of this process. One is that the precursors provided diffuse to the underlying surface with Al catalyst atoms through the space between the previously formed siloxane chains and react with Al atoms by breaking the Al−O bonds (Figure 1c). This film growth looks like that the height of the blocks increases by inserting new blocks at the bottom positions. The other is that the reaction continues until the diffusion path of the precursors is blocked by cross-linking between hydroxyl groups bonded to Si atoms in the siloxane chains (Figure 1d). Hydroxyl groups on the silicon atoms are derived from the thermal decomposition of tert-pentoxy groups on the siloxane chains through β-hydrogen elimination of isopentylene. Cross-linking means that hydroxyl groups react with other hydroxyl groups to yield H_2O. The cross-linking blocks the precursor diffusion and eventually saturates the film growth as an ALD reaction does. When the precursor diffusion is blocked and film growth is stopped, the film growth can be triggered again by the formation of a new Al catalyst layer on this growth-saturated SiO_2 layer and a subsequent pulse of the Si-precursor. Hausmann et al. reported that the reaction is similar to ALD in two aspects; one is the saturated thickness with respect to the TBS and TMA doses, and the other is the temperature window, from 225 to 250 °C, where the growth rate is constant.[16] The mass density of the film was not too low and the film quality was useful to be adopted in several applications. Burton et al.

Received: February 9, 2011
Accepted: April 25, 2011
Published: April 25, 2011

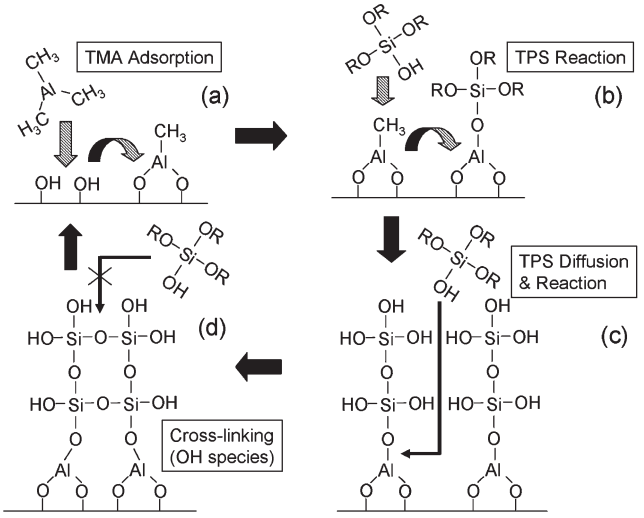

Figure 1. Illustration with four steps showing the growth mechanism of RALD SiO_2.

subsequently reported the similar thickness saturation behaviors using quartz crystal microbalance analysis and a liquid Si-precursor, (*tert*-pentoxy)silanol (TPS), which is more useful than TBS in terms of mass production.[17] The film density increased slightly at higher growth temperatures but the growth rate decreased sharply over 150 °C. The high growth rate can be maintained at a little higher growth temperatures when the partial pressure of TPS increases. A maximum growth rate of ~17 nm/cycle was obtained.[17]

RALD SiO_2 can be used in many semiconductor device applications such as a sacrificial layer for the fabrication of capacitor storage nodes in dynamic random access memory devices, hard mask layer for self-aligned double patterning technology in flash memory devices, gap-fill oxide for shallow trench isolation, gate spacers, protective coatings, and insulating layers in "through silicon via".[18−21] In these applications, the low growth temperature, high growth rate, and excellent step coverage of RALD SiO_2 play an important role. However, further research is required to improve the oxide quality for several critical applications, such as gate spacers. In addition, optimization of the pulse and purge times should be carried out to confirm the more practical (engineering) growth rate in terms of thickness per minute not thickness per cycle. In particular, considering the relation between growth temperature and oxide quality, the sharp decrease in growth rate at higher growth temperatures would be a serious problem. This paper reports the effect of the catalyst layer density on the growth rate using a liquid Si source, TPS, and how TPS pulse times showing saturated growth rates change with increasing growth temperature. In addition, it was shown that an in situ plasma treatment also contributes to the improvement of the film quality.

EXPERIMENTAL SECTION

RALD-SiO_2 thin films were deposited on 4- and 6-in. diameter silicon wafers in a commercially available ALD system (ASM Genitech Corp.) using TPS and TMA. The reaction volume of the chamber was only ~150 cubic centimeters. The reaction chamber has a showerhead which is heated to 120 °C to prevent the precursors from condensation. The chamber wall was heated to the same temperature. TPS was provided to the reaction chamber by a bubbling technique using Ar carrier gas with a flow rate of 50 standard cubic centimeters per minute (sccm). The deposition pressure was 0.6 Torr at the purge steps. A total Ar flow rate of 180 sccm was maintained during all ALD steps. In TMA and TPS pulse steps, the precursor molecules were provided into the chamber with the help of Ar carrier gas flow. A constant carrier gas flow was used so that the precursor was dynamically exposed to the wafer surface. The partial pressure of TPS was 2−3 mtorr when the TPS canister was maintained at 80 °C. The TMA canister was maintained at room temperature and transported into the chamber by the self-vaporization (vacuum draw) without a carrier gas. A metering valve was used at the outlet gas tube of the canister to control the transported amount of TMA. The RALD-SiO_2 thin films were deposited at temperatures ranging from 140 and 230 °C without a reactant gas. The RALD cycle was composed of a TMA pulse (0.02−2 s), TMA purge (4−60 s), TPS pulse (10−110 s), and TPS purge (10−600 s). In some experiments, tetrakis-ethyl-methyl-amino-zirconium (TEMAZ) was pulsed before or after the TMA pulse/purge step to examine the effect of another type of precursor on the catalyst layer. The temperature of the TEMAZ canister was maintained at 60 °C.

The film thickness of SiO_2 was measured by ellipsometry and X-ray reflectivity (XRR). The mass density of SiO_2 was also analyzed by XRR. When TEMAZ was pulsed, the amount of incorporated Zr was estimated by X-ray fluorescence (XRF). The chemical structure of the SiO_2 thin films deposited on *p*-type one-side polished Si wafers was analyzed by normal (transmitted type) Fourier transform infrared (FTIR) spectroscopy. Capacitance density of an ALD SiO_2 film on a Si substrate was measured using a HP4294. The top Pt electrode was fabricated using an e-beam evaporation system through a metal shadow mask. The wet etch rate of RALD-SiO_2 thin films was examined using a 1% HF solution in deionized water. Some RALD-SiO_2 films were treated with either N_2O plasma or O_2 plasma under in situ conditions at the end of each cycle. A 100 nm-thick commercially available thermally grown SiO_2 film was used for the comparison of the wet etching rate with RALD-SiO_2 films.

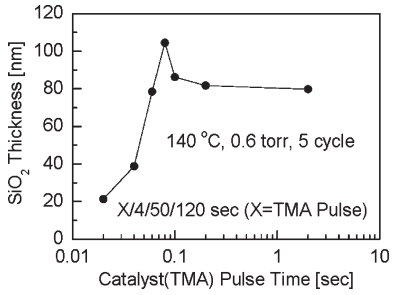

Figure 2. TMA pulse time vs thickness at five cycles showing the effect of the catalyst layer density on the growth rate. TMA/purge/TPS/purge = *X*/4/50/120 s.

RESULTS AND DISCUSSION

Previous reports only showed the TMA pulse times of ≥1 s, which correspond to a fully saturated dose. In this study, the effect of shorter TMA pulse times on the growth rate of SiO_2 film was examined because the Al catalyst may not form a full monolayer even with the saturated dose and the cross-linking reaction can depend on the density of the Al catalyst. In the experiment, TMA purge, TPS pulse, and TPS purge were fixed at 4, 50, and 120 s, respectively, while the TMA pulse time varies. As shown in Figure 2, when the pulse time of TMA varied from 0.02 to 2 s, the maximum growth rate (~23 nm/cycle) was obtained at 0.08 s. Below this TMA pulse time, the growth rate sharply dropped, and over that time, it was saturated at ~18 nm/cycle.

Table 1. Thicknesses and Mass Densities of the RALD-SiO_2 Films with Three Different TMA Pulse Times

TMA pulse	ellipsometry thickness (nm)	XRR thickness (nm)	XRR density (g/cm^3)
0.02 s	21.4	19.8	1.96
0.04 s	38.8	39.2	1.68
0.2 s	81.7	76.2	2.06

Here, the RALD was performed by five cycles. The underdosing condition of an ALD process generally invokes concerns on the nonuniformity of the growing films. However, this concern could be mitigated by the optimized reactor design for the uniform supply of the precursors over the entire wafer surface. The adoption of showerhead type chamber geometry in this experiment allowed the authors to achieve reasonable uniformity to perform the experiment even under the underdosing conditions of TMA in Figure 2. The maximum growth rate was calculated by dividing the film thickness by 4.5 considering that there is an incubation effect which reduces the growth rate of the first cycle to 50% of normal growth rate as shown in the inset of Figure 7a. The increase in growth rate when the TMA pulse time decreases from 0.2 to 0.08 s is probably because the cross-linking reaction becomes slower due to the longer distance between neighboring hydroxyl groups of the siloxane chains at such a lower Al catalyst density. Therefore, more Si-precursor molecules diffuse down to the Al-catalyst layer and form a thicker SiO_2 layer. The growth rate could be even higher at ~0.07 s of TMA pulse time considering the data trend in Figure 2. However, the experimental accuracy of controlling the TMA pulse time with the span of 0.01 s was skeptical with the present experimental setup. Therefore, another method was adopted to further precisely control the TMA adsorption and accompanying TPS adsorption as shown later.

In order to understand the reason for the sharply decreased growth rate under the TMA pulse time of 0.08 s, XRR analysis was performed. As summarized in Table 1, the thicknesses of the SiO_2 films grown at TMA pulse times of 0.02, 0.04, and 0.2 s were confirmed again by XRR spectra. When the TMA pulse time is 0.2 s, the film density is ~2 g/cm^3, which corresponds to the highest density that can be obtained from this experiment. This indicates that the TPS molecules adsorbed densely on the compactly formed TMA catalysts. As the TMA pulse time decreases to 0.04 s, the TMA catalyst density becomes quite low and siloxane chains form only sparsely during the TPS pulse step, leaving voids between them. In the subsequent TMA pulse step, it can be hypothesized the TMA molecules adsorb not only on the top region but also on the side area of the siloxane chains and also on the uncovered bottom surface (Figure 3). Therefore, in the next TPS pulse step, siloxane chains start to grow on these newly formed catalyst molecules. Among these newly formed siloxane chains, the ones growing laterally on the side area of the previously formed siloxane chains blocks the fluent diffusion of TPS molecules into the void region. This eventually decreases the film density as well as the growth rate. As the TMA pulse time further decreases to 0.02 s, the density of siloxane chains formed during the first TPS pulse step decreases further. As in the case of TMA pulse time of 0.04 s, TMA catalyst forms all over the exposed area. Then, the subsequent TPS pulse step forms the siloxane chains again. However, it can be hypothesized that TPS flux into the voids between the previously formed siloxane chains

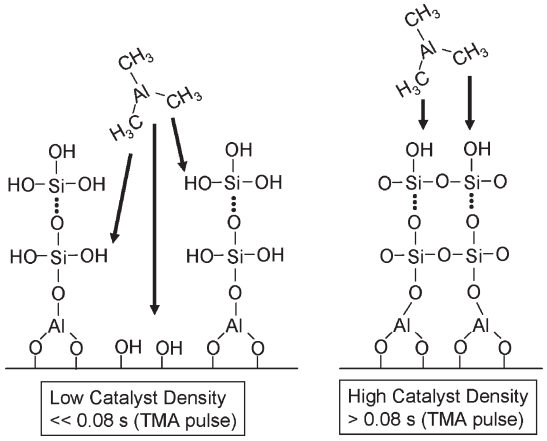

Figure 3. Illustration showing where next-pulsed TMA precursors react in the cases of low and high Al catalyst densities at a previous cycle.

becomes more fluent in this case compared to the case of TMA pulse time of 0.04 s as the space blocking effect by the sideway grown siloxane chains decreases due to its more open structure. This open structure allows the more fluent diffusion of TPS molecules to the bottom region which leads to a more effective refilling of the voids. This can induce an increased film density, as shown in Table 1. It must be noted that the overall growth rate must be much smaller due to the generally inefficient adsorption of TPS on the very limited amount of TMA catalysts provided as the TMA pulse time decreases <0.08 s.

On the other hand, TEMAZ was pulsed and purged instead of TMA to determine if other organo-metallic precursors can be used as a catalyst.[22−24] However, SiO_2 films were barely deposited when using TEMAZ as a catalyst. Furthermore, as shown in Figure 4a, when TEMAZ is pulsed onto the Al catalyst layer, the thickness of the SiO_2 grown by TPS decreased sharply with increasing the TEMAZ pulse time. Here, growth temperature and pressure were 140 °C and 0.6 Torr, respectively. The TEMAZ was pulsed after the TMA pulse (2 s) and purge (4 s) steps at each cycle. After the TEMAZ pulse step, a TEMAZ purge step (4 s) was introduced. TPS pulse and purge times were 50 and 120 s, respectively. It appears that the catalytic activity of TMA for the SiO_2 deposition was destroyed by the TEMAZ pulse of which mechanism is not clearly understood yet.

Inversely utilizing no catalytic growth of SiO_2 on the TEMAZ treated surface, the optimized Al catalyst density could be obtained by the change of the pulse sequence of TMA and TEMAZ. When TEMAZ was pulsed for an appropriate pulse time with an underdosed condition (here, 0.1 s) and then TMA was pulsed onto the vacant reaction sites even for a long TMA pulse time, a very high growth rate of ~28 nm/cycle, which was a little higher than the growth rate (~23 nm/cycle) at the TMA pulse time of 0.08 s, was obtained from the slope of the thickness vs cycle number graph (Figure 4b). This is believed to be due to the optimized distribution of adsorbed TMA molecules for the maximum adsorption TPS without the adverse too sparse TMA effect. From these results, it is certain that the growth rate of >25 nm/cycle in the RALD of SiO_2 can be obtained by the precise control of the TMA amount as a catalyst.

The effect of purge times on the growth rate was also investigated. Figure 5a shows the change of SiO_2 thickness with TMA purge times. The SiO_2 films were grown at the condition of 140 °C, 0.6 Torr, and five cycles. TMA pulse, TPS pulse, and TPS

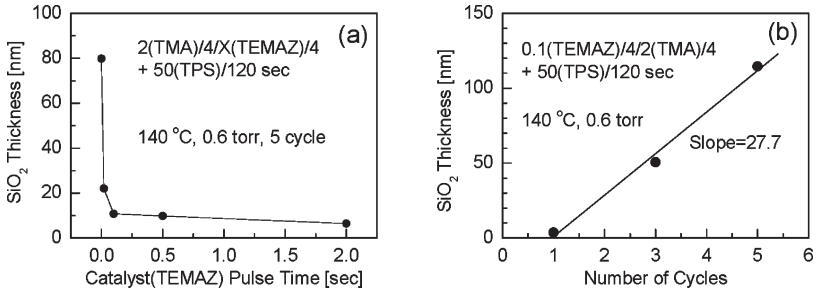

Figure 4. (a) RALD-SiO_2 film thickness as a function of the TEMAZ pulse time after a TMA pulse/purge. (b) Growth rate (~28 nm/cycle) in the case of a TMA pulse (2 s) after a proper TEMAZ pulse time (here, 0.1 s).

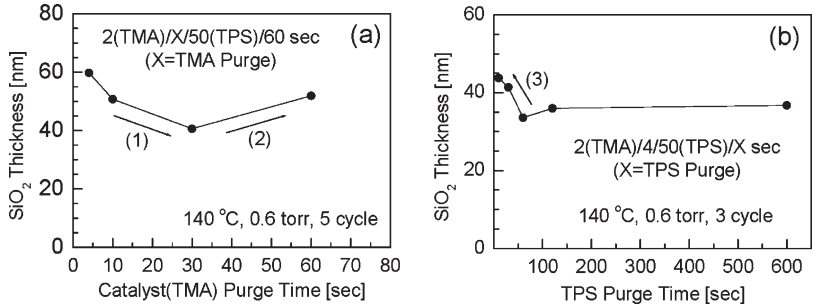

Figure 5. (a) Effect of a TMA purge times on the growth rate. (b) Effect of the TPS purge time on the growth rate.

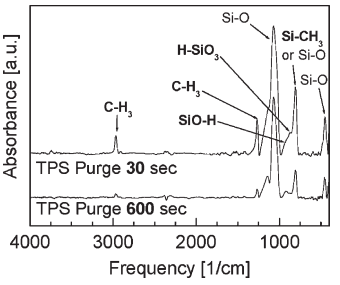

Figure 6. FTIR spectra of RALD-SiO_2 films grown at short (30 s) and long (600 s) TPS purge times.

purge times were fixed at 2, 50, and 60 s, respectively. In the case of the Al_2O_3 growth, the growth rate of Al_2O_3 is saturated at a sufficient TMA purge time. However, as shown in Figure 5a, the film thickness of SiO_2 decreased further at a TMA purge of 30 s and increased again at a TMA purge of 60 s. This phenomenon was also observed in the case of 1 cycle. (data not shown) Even though further studies are required, the reasons for regions 1 and 2 in Figure 5a may be related to the time-dependent change in the adsorption status of the Al catalysts because the growth rate of SiO_2 would be very sensitive to the chemical status of Al catalysts in the RALD SiO_2. Figure 5b shows the change of SiO_2 thickness with TPS purge time. The SiO_2 films were grown at the condition of 140 °C, 0.6 Torr, and three cycles. TMA pulse, TMA purge, and TPS pulse times were fixed at 2, 4, and 50 s, respectively. The saturation behavior was observed in the case of long TPS purge times, whereas thicker films were obtained at too short purge times (region 3 in Figure 5b).

Figure 6 shows FTIR spectra of RALD SiO_2 films grown at short (30 s) and long (600 s) TPS purge times. The growth temperature, pressure, and cycle number were 140 °C, 0.6 Torr, and three cycles. TMA pulse, TMA purge, and TPS pulse times were 2, 4, and 50 s. In the case of a short purge time, a small SiO−H peak (~920 cm^{-1}), a H−SiO_3 peak (~890 cm^{-1}), a very strong Si−CH_3 peak (~800 cm^{-1}), and strong C−H_3 peaks (~1260 and ~2965 cm^{-1}) were observed.[23,26] This is due to the residual byproduct or unreacted precursors which cannot escape from the film because of the insufficient purge time. The result shows that the TPS purge time needs to be more than 60 s to obtain an appropriate film with a low impurity concentration.

For the next stage, the effect of the TPS pulse times on the growth rate of SiO_2 was examined at three growth temperatures (140, 185, and 230 °C). The process pressure and cycle number were 0.6 Torr and three (or five) cycles. And, the TMA pulse, TMA purge, and TPS purge times were fixed at 2, 4, and 120 s, respectively. As shown in Figure 7a−c, the film thicknesses were saturated at approximately 30 s for 140 °C, 70 s for 185 °C, and 90 s for 230 °C. This result is in contrast to a previous report,[17] where the TPS pulse time with a saturated growth rate became short when the growth temperature was increased to >150 °C due to rapid cross-linking. In these experiments, cross-linking was rather delayed at higher growth temperatures. More accurate growth rates were extracted from the slope of the thickness vs number of cycles graphs at TPS pulse times with saturated growth rates. The inset graphs in Figure 7a−c confirmed that the growth rate did not decrease significantly with increasing growth temperature. According to the previous report,[17] the growth temperature at which a high growth rate can be obtained increased with increasing partial pressure of TPS (for example, from 25 to 40 mtorr). In this experimental system, TPS was transported by bubbling of carrier Ar (50 sccm). Vaporization is normally enhanced by bubbling. Therefore, TPS partial pressure of the present experiment may be higher than that of self-vaporization used in the previous report,[17] which may constitute the reason for the discrepancy. However, another effect was

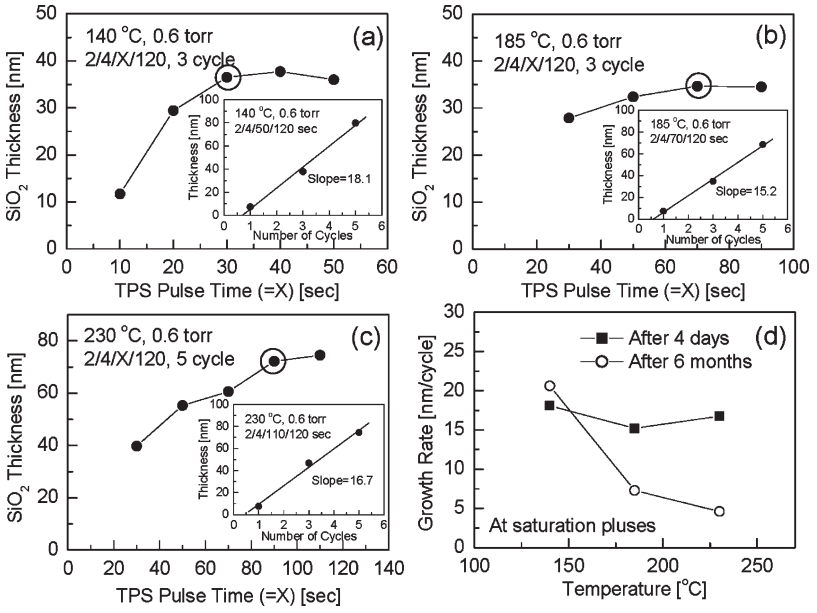

Figure 7. TPS pulse time vs thickness at (a) 140, (b) 185, and (c) 230 °C. The inset graphs show of number of cycles vs thickness. (d) Growth rate as a function of the growth temperature after 4 days and 6 months from the initial heating of the canister.

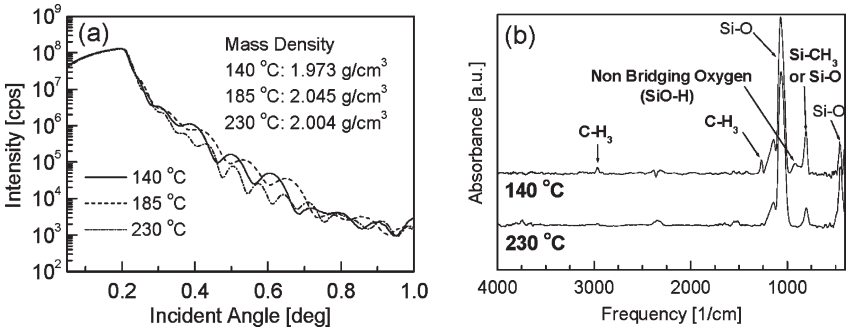

Figure 8. (a) XRR spectra of the RALD-SiO_2 films grown at three different growth temperatures. (b) FTIR spectra of RALD-SiO_2 films grown at 140 and 230 °C.

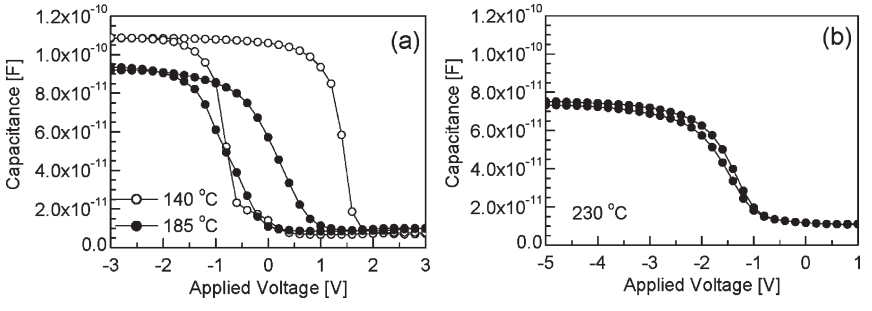

Figure 9. *C*−*V* curves of RALD SiO_2 grown at three different growth temperatures: (a) 140 and 185 and (b) 230 °C.

observed. As shown in Figure 7d, the growth rate decreased drastically with increasing growth temperature after 6 months from the time the source was initially heated. In these experiments, the canister was heated to 40 °C during the downtime and to 80 °C during the process. The partial pressure was not changed even after the 6 months experiment. As the growth temperature increases, the cross-linking reaction will be faster but the diffusion rate of the precursors will also increase. This means that the saturated growth rate will be determined by the competition between the cross-linking rate and the diffusion rate. When a TPS source was maintained at a certain temperature, which is even below the decomposition temperature, for a long time, some of TPS molecules would become a dimer (or even polymer) due to its unstable hydroxyl groups. In the

case of TPS precursors with a dimer type, the increase in the diffusion rate will become lower than that in the cross-linking rate at a higher growth temperature due to the bulky structure of the precursors. In addition, even small amount (less than a few percent) of TPS precursors with a dimer type might block the paths for the diffusion of TPS precursors with a monomer type, while the vapor pressure of the TPS was minimally influenced by the dimerization. Therefore, the saturated growth rate will decrease significantly with increasing the growth temperature. In a fresh precursor condition, however, all TPS molecules exist as a monomer type so that the diffusion rate increases more rapidly than the cross-linking rate as the growth temperature increases. This was confirmed from the data set achieved from the TPS precursor exposed to heat only for 4 days (Figure 7d) As a result, the growth rate does not decrease and the TPS pulse time with a saturated growth rate increases.

Figure 8a shows the results of XRR analysis of the ALD-SiO_2 films grown at three different temperatures. The process pressure was 0.6 Torr. In the samples grown at 140, 185, and 230 °C, cycle numbers were three, three, and five cycles and TMA pulse/TMA purge/TPS pulse/TPS purge times were 2/4/40/120, 2/4/70/120, and 2/4/50/120 s, respectively. The film densities were similar (~2 g/cm^3) at the three different temperatures. The film density of thermally grown oxide was estimated to be 2.2−2.3 g/cm^3 when the same XRR was used. Figure 8b displays the FTIR spectra of the SiO_2 films grown at 140 and 230 °C. In the spectrum of the sample grown at 230 °C, Si−CH_3 and C−H_3 peaks centered at 800, 1260, and 2965 cm^{-1}, and an SiO−H nonbridging oxygen (NBO) peak centered at 920 cm^{-1} almost disappeared,[27,28] while the film grown at 140 °C revealed traces of Si−CH_3 and C−H_3 peaks. This may correspond to the slightly lower density of that film compared to the other as shown in Figure 8a.

Figure 9a and b show capacitance−voltage ($C-V$) curves of RALD SiO_2 grown at three different growth temperatures. Voltage was swept first from a negative voltage to a positive one and then reversely. Electrical properties obtained from the $C-V$ curves are summarized in Table 2. Voltage difference between forward and reverse sweeps (ΔV) was measured at the 50% position of normalized capacitance in $C-V$ curves. ΔV of RALD SiO_2 films became much small as the growth temperature increased. In particular, the SiO_2 film grown at 230 °C showed the very small value of 0.13 V. The defects in the SiO_2 film are the cause of ΔV. The defects would be the Si−OH and Si−CH_3 species which remain due to the incomplete cross-linking reaction. The thickness in Table 2 indicates physical thickness measured by ellipsometry. Capacitance equivalent thickness (CET) was calculated from the maximum capacitance value in $C-V$ curves. The dielectric constant (ε_r) was calculated from the equation of 3.9(thickness/CET). ε_r of the films grown at lower temperatures is much larger than the ideal value of SiO_2 (3.9), but it became closer to 3.9 as the growth temperature increased. This is probably related to the reduced amount of the Si−OH species.

Table 2. Summary of Electrical Properties Obtained from the *C*−*V* Curves of Figure 9

	thickness (nm)	CET (nm)	ε_r	ΔV (V)
140 °C	36.5	22.3	6.38	2.25
185 °C	34.5	25.9	5.19	0.95
230 °C	39.7	32.7	4.73	0.13

Figure 10a and b show the wet etch rates in the HF 1% solution of the ALD-SiO_2 films grown under various growth conditions. The wet etch rate test is a viable method to evaluate the relative density of the various SiO_2 films. The wet etch rate increased with an increasing growth rate, even at the same growth temperature (Figure 10a). Numbers 1 and 2 with higher growth rates compared to number 3 showed a ~30% higher wet etch rate. Number 1 was deposited at the TMA pulse and purge times of 0.08 and 4 s, respectively. Number 2 was made in the condition that TEMAZ pulse, TEMAZ purge, TMA pulse, and TMA purge times were 0.1, 4, 2, and 4 s, respectively. In numbers 1 and 2, TPS pulse and TPS purge times were 50 and 120 s, respectively. TMA pulse, TMA purge, TPS pulse, and TPS purge times in number 3 were 2, 4, 50, and 120 s. A comparison of number 3−5 showed that the wet etch rate decreases with increasing growth temperature, but the amount was not large (~27%). However, as shown in Figure 10b, the in situ O_2-plasma treatment (100 W, 30 s) per cycle greatly reduced the wet etch rate (~38%). For this plasma treatment experiment, the plasma application step was added at the end of every deposition cycle. There was no notable change in the growth rate by the addition of the plasma steps. The lowest wet etch rate in these experiments was obtained from the sample treated with the N_2O plasma (100 W, 30 s), which was ~3.5 times (7.5 nm/min) higher than that (2.2 nm/min) of the thermally grown oxide. This is a very striking value considering the growth temperature was only 230 °C. This suggests that the in situ plasma application is a viable method to improve the film density even at such a low temperature.

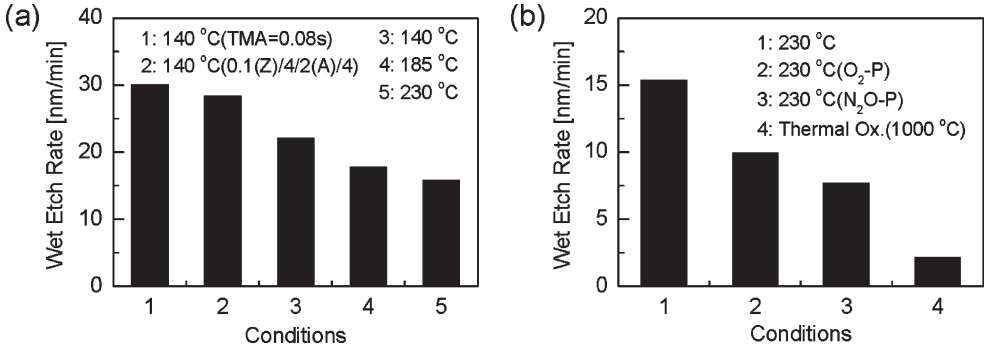

Figure 10. Wet etch rates in HF 1% evaluated under various growth and annealing conditions showing the effect of (a) catalyst layer density and growth temperature and (b) post-treatments compared to the thermally grown oxide.

CONCLUSIONS

Silicon oxide films were deposited by ALD using TPS as the silicon source and TMA as the catalyst without any reactant gases. A very high growth rate of ~28 nm/cycle was obtained by controlling the Al catalyst layer density. This is a much higher value than ever reported for ALD. In contrast to a previous report, the growth rate did not decrease even at a high growth temperature of 230 °C and the TPS pulse time with a saturated growth rate became rather longer. This is probably because the diffusion rate of the TPS precursor increases faster than the cross-linking rate of hydroxyl groups with increasing the growth temperature. Undesirable Si−CH_3, Si−OH, and Si−H bonds almost completely disappeared in the ALD silicon oxide film grown at 230 °C. An in situ O_2-plasma or N_2O-plasma treatment per cycle greatly reduces the wet etch rate suggesting the improved film quality. It is anticipated that a higher growth rate and excellent film quality can be obtained at higher growth temperatures when a liquid delivery system with a vaporizer is adopted because the precursor can be maintained under fresh conditions for a long time with this experimental setup.

AUTHOR INFORMATION

Corresponding Author

*E-mail: thinfilm@snu.ac.kr (H.J.K.) cheolsh@snu.ac.kr (C.S.H.).

ACKNOWLEDGMENT

This study was supported by the Korea Science and Engineering Foundation (KOSEF) grant funded by the Korea government (MEST) (No. R17-2008-043-01001-0), the Converging Research Center Program through the National Research Foundation of Korea (2010K000977), and World Class University program through the Korea Science and Engineering Foundation funded by the Ministry of Education, Science and Technology (R31-2008-000-10075-0).

REFERENCES

(1) Puurunen, R. L. *J. Appl. Phys.* **2005**, *97* (121301), 1–52.
(2) Leskelä, M.; Ritala, M. *Thin Solid Films* **2002**, *409*, 138–146.
(3) Lim, B. S.; Rahtu, A.; Gordon, R. G. *Nat. Mater.* **2003**, *2*, 749–754.
(4) Kim, S. K.; Lee, S. W.; Hwang, C. S.; Min, Y.-S.; Won, J. Y.; Jeong, J. *J. Electrochem. Soc.* **2006**, *153* (5), F69–F76.
(5) Gordon, R. G.; Hausmann, D.; Kim, E.; Shepard, J. *Chem. Vap. Deposition* **2003**, *9* (2), 73–78.
(6) Elam, J. W.; Routkevitch, D.; Mardilovich, P. P.; George, S. M. *Chem. Mater.* **2003**, *15*, 3507–3517.
(7) Houssa, M.; Pantisano, L.; Ragnarsson, L.-Á.; Degraeve, R.; Schram, T.; Pourtois, G.; De Gendt, S.; Groeseneken, G.; Heyns, M. M. *Mater. Sci. Eng. R.* **2006**, *51*, 37–85.
(8) Kim, S. K.; Choi, G.-J.; Lee, S. Y.; Seo, M.; Lee, S. W.; Han, J. H.; Ahn, H.-S.; Han, S.; Hwang, C. S. *Adv. Mater.* **2008**, *20*, 1429–1435.
(9) Lim, B. S.; Rahtu, A.; De Rouffignac, P.; Gordon, R. G. *Appl. Phys. Lett.* **2004**, *84* (20), 3957–3959.
(10) de Rouffignac, P.; Li, Z.; Gordon, R. G. *Electrochem. Solid-State Lett.* **2004**, *7* (12), G306–G308.
(11) Liu, X.; Deng, X.; Paul Sciortino, J.; Buonanno, M.; Walters, F.; Varghese, R.; Bacon, J.; Chen, L.; O'Brien, N.; Wang, J. J. *Nano Lett.* **2006**, *6* (12), 2723–2727.
(12) Wang, J. J.; Deng, X.; Varghese, R.; Nikolov, A.; Sciortino, P.; Liu, F.; Chen, L. *Opt. Lett.* **2005**, *30* (14), 1864–1866.
(13) Wang, J. J.; Deng, X.; Varghese, R.; Nikolov, A.; Sciortino, P.; Liu, F.; Chen, L.; Liu, X. *J. Vac. Sci. Technol. B* **2005**, *23*, 3209–3213.
(14) Wang, J. J.; Liu, F.; Deng, X.; Liu, X.; Chen, L.; Sciortino, P.; Varghese, R. *J. Vac. Sci. Technol. B* **2005**, *23*, 3164–3167.
(15) Dameron, A. A.; Davidson, S. D.; Burton, B. B.; Carcia, P. F.; McLean, R. S.; George, S. M. *J. Phys. Chem. C* **2008**, *112*, 4573–4580.
(16) Hausmann, D.; Becker, J.; Wang, S.; Gordon, R. G. *Science* **2002**, *298*, 402–406.
(17) Burton, B. B.; Boleslawski, M. P.; Desombre, A. T.; George, S. M. *Chem. Mater.* **2008**, *20*, 7031–7043.
(18) Park, J.-E.; Ku, J.-H.; Lee, J.-W.; Yang, J.-H.; Chu, K.-S.; Lee, S.-H.; Park, M.-H.; Lee, N.-I.; Kang, H.-K.; Suh, K.-P. *IEDM Tech. Dig.* **2002**, 229–232.
(19) Lu, H.; Cui, H.; Bhat, I.; Murarka, S.; Lanford, W.; Hsia, W.-J.; Li, W. *J. Vac. Sci. Technol. B* **2002**, *20* (3), 828–833.
(20) Andry, P. S.; Tsang, C. K.; Webb, B. C.; Sprogis, E. J.; Wright, S. L.; Dang, B.; Manzer, D. G. *IBM J. Res. Dev.* **2008**, *52* (6), 571–581.
(21) Lee, S.-W.; Joo, S.-K. *IEEE Electr. Dev. Lett.* **1996**, *17* (4), 160–162.
(22) Zhong, L.; Zhang, Z.; Campbell, S. A.; Gladfelter, W. L. *J. Mater. Chem.* **2004**, *14*, 3203–3209.
(23) Liu, J.; Lennard, W. N.; Goncharova, L. V.; Landheer, D.; Wu, X.; Rushworth, S. A.; Jones, A. C. *J. Electrochem. Soc.* **2009**, *156* (8), G89–G96.
(24) Zhong, L.; Chen, F.; Campbell, S. A.; Gladfelter, W. L. *Chem. Mater.* **2004**, *16*, 1098–1103.
(25) Wang, Y. H.; Moitreyee, M. R.; Kumar, R.; Shen, L.; Zeng, K. Y.; Chai, J. W.; Pan, J. S. *Thin Solid Films* **2004**, *460*, 211–216.
(26) Grill, A.; Neumayer, D. A. *J. Appl. Phys.* **2003**, *94* (10), 6697–6707.
(27) Teshima, K.; Inoue, Y.; Sugimura, H.; Takai, O. *Surf. Coat. Technol.* **2001**, *146−147*, 451–456.
(28) Yin, Z.; Tsu, D. V.; Lucovsky, G; Smith, F. W. *J. Non-Cryst. Solids* **1989**, *114*, 459–461.